

Heat-Transfer and Pressure Drop Experiments in Air-Cooled Electronic-Component Arrays

P. R. Souza Mendes*

Pontifícia Universidade Católica do Rio de Janeiro, Rio de Janeiro, Brazil

and

W. F. N. Santos†

Instituto de Pesquisas Espaciais, Cachoeira Paulista, Brazil

An experimental investigation to determine the effect of geometrical nonuniformities on heat transfer and pressure drop of arrays of rectangular modules deployed along one wall of a parallel-plate channel is performed. The presence of a taller module in the array and its consequences on heat-transfer coefficients of other modules are investigated for various relative positions of the taller module, including both the entrance and the fully developed portions of the airflow. The heat-transfer coefficients at the tall module are also measured for different values of the Reynolds number and relative positions in the array. Among other findings, it is observed that the heat-transfer coefficients of the two modules siding the tall module display the highest enhancements.

Nomenclature

A	= surface area of mass transfer
D	= diffusion coefficient
H	= clearance height, Fig. 1
K	= per-module mass-transfer coefficient
L	= side of square module, Fig. 1
\dot{m}	= air mass flow rate
\dot{M}	= mass-transfer rate at module
Nu	= Nusselt number
p	= static pressure
p_{atm}	= barometric pressure
p_{nw}	= naphthalene vapor pressure
Pr	= Prandtl number
R	= gas constant of naphthalene vapor
Re	= Reynolds number
S	= intermodule gap
Sc	= Schmidt number
Sh	= Sherwood number
$Sh_{fd,r}$	= fully developed value of Sh for the uniform array
$Sh_{fd,t}$	= fully developed value of Sh for the tall module
t	= height of regular module, Fig. 1
T	= absolute temperature of module surface
V	= characteristic velocity
W	= spanwise width of array
x	= axial coordinate, measured from the entrance of the developing section
ΔM	= corrected mass that sublimed during the data run
Δp_{incr}	= incremental pressure drop associated with the tall module
μ	= air absolute viscosity
ν	= air kinematic viscosity
ρ	= air density
ρ_{nb}	= bulk density of naphthalene vapor
ρ_{nw}	= density of naphthalene vapor at module surface
τ	= time duration of data run

Introduction

EFFICIENT design of cooling systems for electronic equipment is still a challenging task for engineers. This happens mainly due to dearth of related heat-transfer information. Presently, it seems that most designers still rely on heat-transfer data obtained for physical models that are too far from the complex configurations found in electronic equipment.¹

A pioneer study of a configuration that more closely meets the actual physical situation is presented by Sparrow et al.² This remarkable paper reports on forced convection, heat-transfer measurements in an array of heat-generating modules of uniform size and shape situated in a parallel-plate channel. The effect on heat transfer and pressure drop of missing components and heat-transfer-enhancing barriers is also investigated, and an extension of this study is presented in Ref. 3.

Upon examination of the interior of any electronic equipment, it is readily seen that the electronic components are far from being uniform in size and shape. This fact greatly complicates any attempt to develop a physical model that is close enough to the real heat-transfer situation and, at the same time, is amenable to conclusive experimental analysis.

The first work that tackled this unusually involved problem is reported in Ref. 4, where the heat-transfer response to the occasional presence of modules whose height differs from that of the others in the array was investigated. The work just mentioned was concerned with the part of the array in which fully developed flow would prevail if the odd-size modules were not present.

The work reported here investigates the effect of a geometrical nonuniformity on forced convection heat transfer and pressure drop in an array of modules in a flat rectangular duct. The nonuniformity investigated consisted of a module whose height was twice the height of the other modules in the array. This tall module was positioned at different locations in the array, and the effect of its presence on heat transfer was quantified, both for the entrance and fully developed regions of the flow. Pressure drop measurements were also performed for different mass flow rates.

Experiments

The physical situation reproduced in the laboratory was the forced convection flow in a parallel-plate channel. The walls

Received April 10, 1986; presented as Paper 86-1301 at the AIAA/ASME 4th Thermophysics and Heat Transfer Conference, Boston, MA, June 2-4, 1986; revision received Dec. 19, 1986. Copyright © American Institute of Aeronautics and Astronautics, Inc., 1987. All rights reserved.

*Associate Professor, Mechanical Engineering Department.

†Researcher, Department of Energy.

were adiabatic, and an array of rectangular heat-generating modules was deployed along one of the channel walls (Fig. 1). All modules were of equal dimensions, except one, which was twice as tall as the others. The location of this tall module was varied, and its heat-transfer coefficient was measured as well as the coefficients of all the other modules.

Although the heat-transfer situation described in the preceding paragraph was the subject of the present experimental investigation, no heat-transfer experiments were performed. As a matter of fact, one of the main concerns during the experiments was to eliminate all temperature gradients in the laboratory. The desired heat-transfer coefficients were measured with the aid of the well-known naphthalene sublimation technique, which is based on the existing analogy between heat- and mass-transfer mechanisms. Therefore, only mass-transfer experiments were performed.

The channel walls were metallic (no mass transfer) and, for each position of the tall module (also metallic), the heat (mass)-transfer coefficients of the other modules were determined as follows. One of the metallic modules in the array was substituted by a naphthalene module of identical dimensions (specially fabricated for this application), and then the flow in the channel was activated. With knowledge of the amount of sublimation in the naphthalene module (and of other relevant information), the transfer coefficient could be determined at that module position. All other relative positions were investigated in the same fashion, and the heat-transfer response to the flow disturbance caused by the presence of the tall module could be determined by comparing the results thus obtained with heat (mass)-transfer results obtained for the uniform array. The transport coefficients at the tall module were also measured by employing the same procedure, and naphthalene tall modules were also fabricated for this specific purpose.

Experimental Apparatus

A rectangular duct with an aspect ratio of 5:1 was the main piece of the experimental apparatus. Its cross-section width was 13.4 cm, height was 2.67 cm. The duct was composed of a 165-cm-long development section followed by a 58.4-cm accessible test section (see Fig. 1) and, downstream of it, an additional 48.3 cm of duct length. All inner surfaces were polished to provide smooth walls.

The bottom surface of the test section was populated with an array of small rectangular brass modules, regularly distributed in 17 rows. Each row was comprised of three center modules and two half-modules, one adjacent to each of the side walls. The idea behind this layout was to model an array of infinite spanwise dimension, and this procedure was shown in Ref. 2 to be satisfactory. Each center module was square in plan view and rectangular in side view, with length $L = 2.67$ cm and height $t = 1.00$ cm ($t/L = 3/8$) for the regular module and twice this height for the tall module. The inter-module gap was $S = 0.67$ cm, such that $S/L = 0.25$. The height measured from the top surface of the module to the top inner surface of the duct was $H = 1.67$ cm. Hence, the total cross-section height ($H + t$) was equal to the module length $[(H + t)/L = 1]$.

All brass modules were removable to allow substitution either by the tall brass module or by a naphthalene module, which was cast in either of the two different dimensions (regular and tall modules). Furthermore, the top surface of the test section was also removable, which permitted ready access

to the modules. The rectangular duct was made of 0.64-cm-thick aluminum walls, except the test section top surface, which was made of plexiglass.

An orifice-type flowmeter was installed downstream of the rectangular duct, followed by a cut-off valve and another valve used to select the flow rate. After the valves, a short pipe crossing the laboratory wall connected the apparatus to two blowers, which were installed in an adjacent room. With this arrangement, the test section worked in a suction mode. Air entered the rectangular duct through a baffle plate, installed at one of its ends, flowed along the hydrodynamical development section, went through the test section, and then through the rest of the open loop.

Pressure taps were installed along the top surface of the duct, in order to allow the pressure drop measurements. There were 23 taps; 12 of them along the test section, four along the developing section, and the rest along the downstream section.

Heat-Transfer Experiments

Before a typical heat-transfer run could be performed, several provisions had to be made. Naphthalene modules were fabricated by employing an efficient casting technique, providing perfectly smooth naphthalene surfaces. After the casting procedure, the modules were wrapped in plastic film to eliminate contact with the environment, and then transported to the laboratory room where the data runs took place.

During the experiments, the temperature of the room was controlled to ensure no temperature changes in the environmental air. Once the naphthalene piece to be used in a data run was in thermal equilibrium with the room air, the run was ready to start. This equilibrium period was approximately 16 h.

The beginning of a data run was preceded by a warming-up period of the blowers, which was necessary to ensure a steady airflow rate. During this period, the naphthalene module was already positioned in the test section, although still wrapped. Then, the blowers were switched off, the naphthalene module was removed, unwrapped, weighed in a high-precision balance, and positioned back in the test section. Immediately after this operation, the test section was closed and the blowers were turned on, marking the start of the data run.

During the data run, several measurements were performed. The air temperature was read at short intervals from a 0.1°C ASTM-certified thermometer, which was located close to the duct entrance. The additional data recorded to allow determination of the airflow rate were the atmospheric pressure, the pressure drop across the orifice plate of the flowmeter, and the pressure upstream of the orifice plate. The run was concluded by closing the cut-off valve, and immediately the module was brought to the balance for a second weighing. During all of these operations, the naphthalene module was never touched with bare hands; rubber gloves were used to avoid contamination and heating.

To estimate the extraneous sublimation that might have occurred before starting and after terminating each data run, the run procedure was then repeated in every detail, except for the fact that the blowers were not activated. This procedure determined a correction for the sublimed mass, which was always very low compared to the total mass transfer.

Pressure Drop Experiments

The static pressure at the taps was measured with the aid of a device capable of measuring pressure differences of the order of 10^{-4} Torr (MKS Instruments, model 310BH-L, with 1 Torr head). This equipment was used in connection with an integrating voltmeter.

The data run procedure was standard, thus no further description is needed. However, it is worth reporting that, due to pressure fluctuations, three measurements at a given tap were made for each mass flow rate investigated, and the mean of the readings was assumed to be the pressure at the tap.

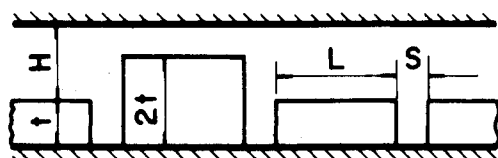


Fig. 1 Test section.

Data Reduction

The mass-transfer data obtained in the experiments were employed in the determination of the per-module mass-transfer coefficients, defined as

$$K = \dot{M} / (A(\rho_{nw} - \rho_{nb})) \quad (1)$$

where

$$\dot{M} = \Delta M / \tau \quad (2)$$

is the mass transfer rate, and ΔM and τ are the corrected sublimed mass and the time duration of the run, respectively. A represents the surface area of mass transfer, whereas ρ_{nw} and ρ_{nb} are the naphthalene vapor densities at the surface module and in the bulk flow, respectively. Since only one naphthalene module was present in the test section during a given data run, ρ_{nb} was simply equal to zero. The quantity was determined from the ideal gas law

$$\rho_{nw} = p_{nw} / RT \quad (3)$$

where p_{nw} is the naphthalene vapor pressure at the module surface and T its absolute temperature. R represents the ideal gas constant for naphthalene vapor, equal to 64.87 J/kg·K.

The following relation⁵ gives the naphthalene vapor pressure as a function of the absolute temperature:

$$\log_{10} p_{nw} = 11.884 - 3729.444/T \quad (4)$$

The Sherwood number was given by

$$Sh = KL/D; \quad D = \nu/Sc \quad (5)$$

In the preceding expressions, D is the mass diffusion coefficient, ν the air kinematic viscosity, and Sc the Schmidt number, equal to 2.5 for the pair naphthalene-air.⁵ The Reynolds number was defined as

$$Re = \rho VH/\mu; \quad V = \dot{m}/\rho HW \quad (6)$$

where ρ and μ are the air density and absolute viscosity, respectively, and V is a characteristic velocity at the flow passage above the modules. It is worth noting that V is not exactly the mean velocity at a given cross section, since HW is not the actual free flow area. The quantity \dot{m} is the total air mass flow rate, and W is the spanwise channel width.

It is worth emphasizing that, according to the analogy between heat and mass transfer, the mass-transfer results are also valid for heat-transfer situations provided $Pr = Sc$ (Pr is the Prandtl number). In such situations, the Nusselt number Nu is equal to the Sherwood number. However, for other interesting values of Pr , especially $Pr = 0.7$, which is the case of heat transfer to air, the results cannot be directly employed. This difficulty is readily removed when the concept of heat/mass transfer analogy is invoked. As discussed in Ref. 2, the Nusselt number for $Pr = 0.7$ can be determined from

$$Nu = 0.632Sh \quad (7)$$

provided the Sherwood number Sh pertains to the case of $Sc = 2.5$. For other fluids, a similar expression can also be obtained.

Uncertainty Analysis

The method of estimating uncertainties in experimental results proposed by Kline and McClintock⁶ was employed in the present work.

The uncertainty associated with the Sherwood number was found to vary in the range 2.4–7.4%. For a regular module, the uncertainty on Sh varied from 3.4% for $Re = 200$ to 5.8% for $Re = 7000$. For a tall module, the corresponding values are 5.6% for $Re = 2000$ and 7.4% for $Re = 7000$.

Results and Discussion

Heat-Transfer Results

Two distinct classes of heat-transfer results will now be discussed. First, the heat (mass)-transfer behavior at the tall module will be focused, and hence attention will be turned to the tall-module influences on heat (mass)-transfer at other (regular) modules.

To allow direct comparison with available results, the Reynolds number values investigated in the present experimental research were 2000, 3700, and 7000.

In order to validate the apparatus and experimental procedure employed, experiments for the regular array were also performed in the present research, and the results obtained ($Sh_{df,r} = 36.82, 57.10, \text{ and } 91.67$ for $Re = 2000, 3700, \text{ and } 7000$, respectively) agree with Ref. 2 to within 5%.

Tall Modules

Refer now to Fig. 2, which illustrates the tall-module Sherwood number at several streamwise locations and for some values of the Reynolds number. It is readily seen that, after the fifth row (for the Reynolds number range under investigation), the Sherwood number becomes independent of the tall-module position, indicating the flow development, both for the regular array and for the tall-module case. As expected, the Sh values for the tall module are higher than for the regular array, since the area exposed to the core flow is larger for the tall module. Furthermore, it can be observed that the entry length mildly decreases with the Reynolds number.

Another interesting finding is that, although for the regular array the entry region is characterized by higher Sherwood

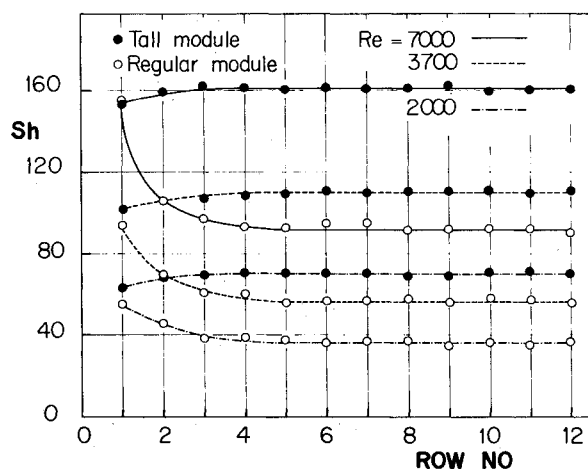


Fig. 2 Sherwood number distributions for the regular and tall modules.

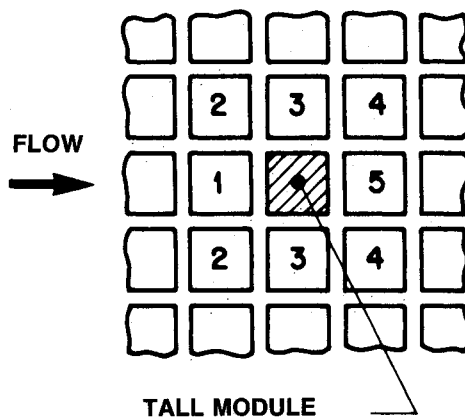


Fig. 3 Labeling the relative positions.

numbers, the opposite is true for the Sh values corresponding to the tall module. This is explained when the two different physical situations are examined more closely.

The heat-transfer rate of a *regular* module at the first row is higher than at subsequent rows due to two reasons. First, the front surface is directly exposed to the flow, which does not happen at the other rows. Second, the side surfaces are still significantly active from the point of view of heat transfer, since the flow through the intermodule gaps, at this point, has velocities of the same order of magnitude as in the core flow above the modules. As the flow resistance through the gaps increases, the air tends to leave the gaps and flow only above the array, yielding higher velocities at the core and very low velocities close to the side surfaces. Hence, very low heat-transfer rates are found at these side surfaces. Therefore, the top surface of a regular module carries almost all of the burden of heat transfer, resulting in a pronounced decrease of the per-module average heat (mass)-transfer coefficient as the flow develops.

A considerably different situation occurs for the *tall* module. In the first row, the tall or regular modules are both exposed to the same flow conditions, and hence the heat-transfer coefficients are very close to each other. In subsequent rows, however, part of the front and side surfaces become nearly inactive as far as heat transfer is concerned, but, on the other hand, the rest of these vertical surfaces and also the top surface become exposed to higher velocities at the

core, increasing heat transfer. The conjunction of these two counteracting effects yields a still positive heat-transfer effect, as can be observed in Fig. 2.

The fully developed Sherwood number at the tall module, $Sh_{fd,t}$, was found to be equal to $Sh_{fd,r} = 71.25$, 110.5, and 161.9 for $Re = 2000$, 3700, and 7000, respectively.

Heat-Transfer Effects Due to the Presence of the Tall Module

Figures 4–9 show how the Sherwood number of a regular module is affected by the proximity of a tall module. In Fig. 3, the relative positions around the tall module are labeled, and, in Figs. 4–9, the Sherwood numbers of regular modules at these relative positions are given as a function of their position in the array (row number).

Upon examination of Figs. 4–9, it can be observed that the largest enhancement of heat transfer is found at position 3, i.e., by the side of the tall module. Enhancements of up to 50% were observed. The second best relative position (as far as heat-transfer enhancement is concerned) is just downstream of the tall module (position 5), with enhancements almost as high as those found at position 3. Position 2 displayed the lowest enhancement, which was of the order of 17%.

It can also be concluded that there is a mild trend to decrease the percentual heat-transfer enhancements as the Reynolds number increases. The relative position most sensitive to Re is position 5, whereas heat-transfer enhancement at position 2 seems to be nearly independent (on a percent basis) of the Reynolds number. As a last comment on these figures, it can be observed that the Sherwood numbers of regular modules at the entry length undergo lower percentual changes.

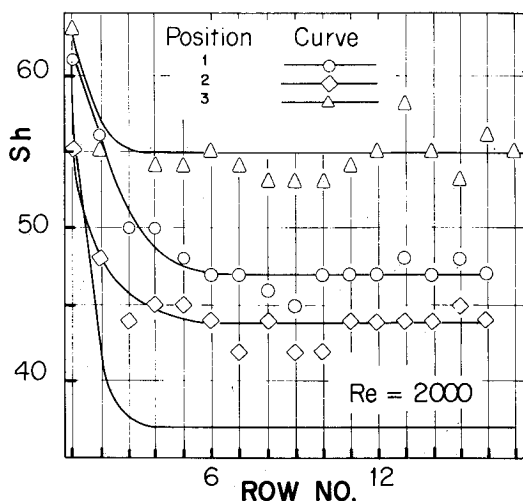


Fig. 4 Influence of the tall module on the Sherwood number of modules around it. $Re = 2000$, positions 1 and 2.

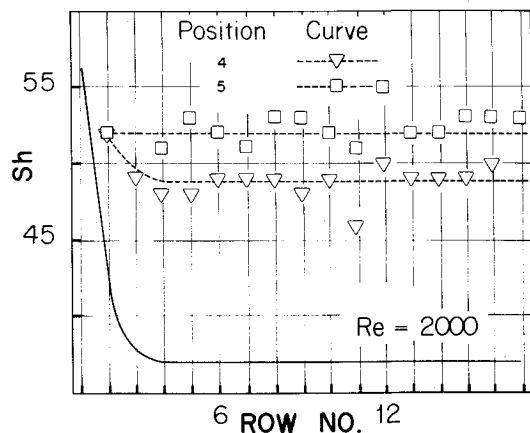


Fig. 5 Influence of the tall module on the Sherwood number of modules around it. $Re = 2000$, positions 3, 4, and 5.

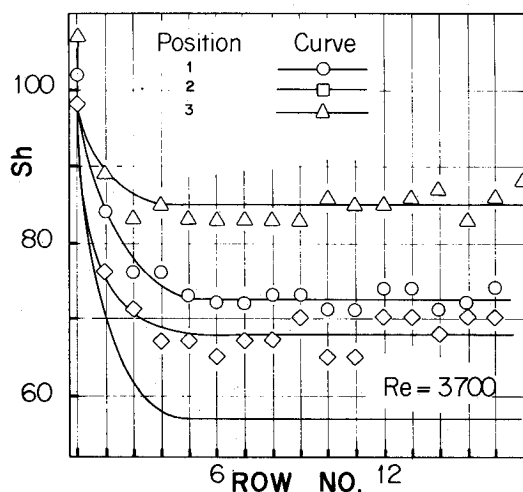


Fig. 6 Influence of the tall module on the Sherwood number of modules around it. $Re = 3700$, positions 1 and 2.

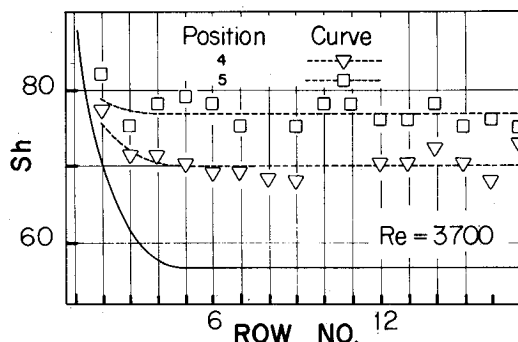


Fig. 7 Influence of the tall module on the Sherwood number of modules around it. $Re = 3700$, positions 3, 4, and 5.

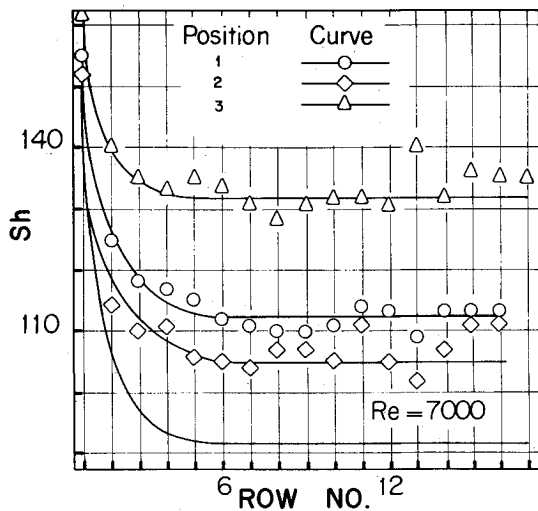


Fig. 8 Influence of the tall module on the Sherwood number of modules around it. $Re = 7000$, positions 1 and 2.

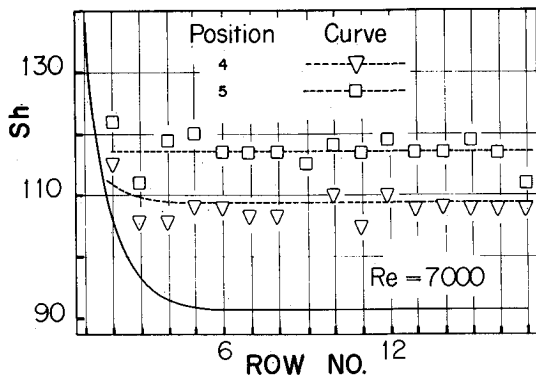


Fig. 9 Influence of the tall module on the Sherwood number of modules around it. $Re = 7000$, positions 3, 4, and 5.

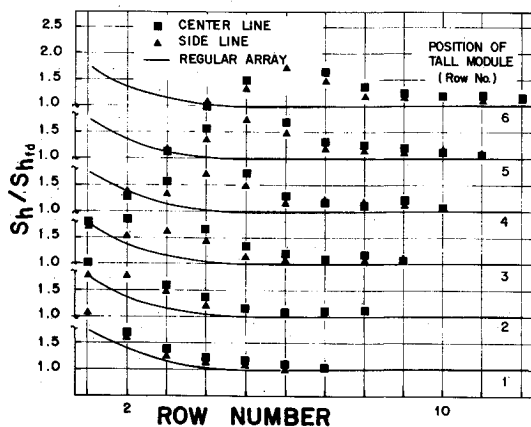


Fig. 10 Range of influence of the tall module on the Sherwood number of other modules. $Re = 2000$.

Heat-transfer effects of the tall module at farther relative positions are, in most situations, not as important as at the relative positions discussed in the foregoing paragraphs. Data for other relative positions can be found in Ref. 7, where an extensive study is presented.

A visualization of the overall effect of the tall module on heat transfer of the array is provided in Fig. 10, which pertains to the case of $Re = 2000$. Other Reynolds numbers are also investigated in Ref. 7, but the strongest influences are represented in Fig. 10.

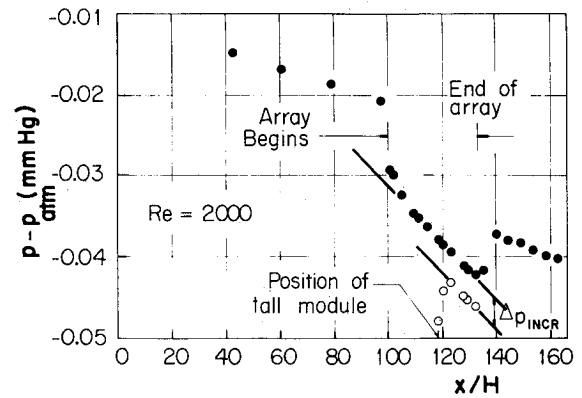


Fig. 11 Incremental pressure drop associated with tall module. $Re = 2000$.

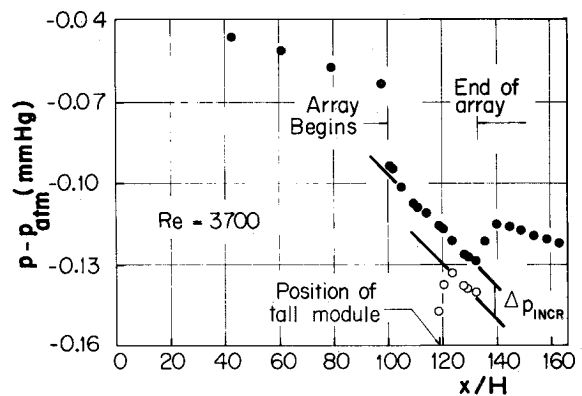


Fig. 12 Incremental pressure drop associated with tall module. $Re = 3700$.

Six curves are presented in this figure, each one for a different fixed position of the tall module. Two different sets of data are given for each curve, one corresponding to Sherwood numbers of regular modules located along the streamwise line where the tall module is positioned, and the other pertaining to Sherwood numbers along the side line.

When the tall module is situated in the first row (curve 1, Fig. 10), its effect on heat transfer at other modules is very mild, and observed only up to the fourth row downstream. As the tall module is displaced downstream, its influences become more significant, spreading farther downstream.

It is also observed that the heat (mass)-transfer enhancement at modules deployed along the side line is always lower than at corresponding modules (same row) along the tall-module line. When the tall module is positioned in the fully developed region of the array (after the fifth row), heat-transfer effects can be felt at the row just upstream and at the following six rows downstream (for $Re = 2000$). For other Reynolds numbers, the effects of the presence of the tall module are milder and are confined to a smaller region in its neighborhood.

Pressure Drop Results

In Figs. 11–13, the axial pressure distributions for arrays with and without a tall module are presented. The quantity Δp_{incr} , indicated in these figures, denotes the incremental pressure drop associated with the presence of a tall module in the array. The black data (\bullet) pertain to the axial pressure distribution along the duct when a uniform array populates the test section. The open data (\circ) represent the pressure distribution in the region of the array that was downstream of the tall module, which was positioned, during the pressure drop measurements, in the tenth row of the array.

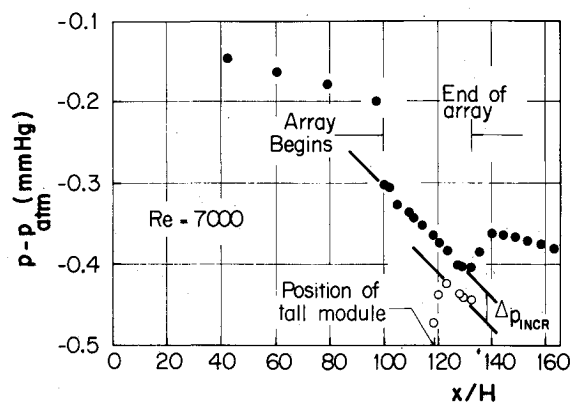


Fig. 13 Incremental pressure drop associated with tall module. $Re = 7000$.

Pressure measurements upstream of the tall module were also made, and these data coincided with the data for the uniform array.

It is observed in any of the three last figures that the flow in the uniform array develops very fast, since the pressure data fall on a negative-slope straight line. When the tall module is present, the pressure drops at its cross section, due to acceleration of the flow. Just downstream of the tall module, the pressure recovers, due to the enlargement of the cross section, and then the flow develops again, the pressure data falling on another straight line. As expected, the two straight lines in any of the three figures are parallel. Furthermore, as indicated in the illustrations, the vertical distance between the lines represents the incremental pressure drop due to the presence of the tall module.

As a last comment on Figs. 11–13, note that the incremental pressure drop associated with a tall module is typically very small, being equivalent, as far as pressure drop is concerned, to about five or six rows of the uniform array.

Concluding Remarks

Experiments were performed to investigate the influence on heat transfer of the presence of nonuniformities in an array of block-like electronic components. It is inferred from the results of the present research that it is very advisable, from the point of view of cooling of electronic components, to explore the effects of these nonuniformities while arranging the components on printed circuit boards. For example, in many instances, it might be advisable to locate a high-power component by the side of a taller component, since, in the present study, heat-transfer enhancements of the order of 50% were measured at this relative position.

References

- ¹Kraus, A. D. and Bar-Cohen, A., *Thermal Analysis and Control of Electronic Equipment*, Hemisphere, Washington, 1983.
- ²Sparrow, E. M., Niethammer, J. E., and Chaboki, A., "Heat Transfer and Pressure Drop Characteristics of Arrays of Rectangular Modules Encountered in Electronic Equipment," *International Journal of Heat and Mass Transfer*, Vol. 25, 1982, pp. 961–973.
- ³Sparrow, E. M., Vemuri, S. B., and Kadle, D. S., "Enhanced and Local Heat Transfer Pressure Drop, and Flow Visualization for Arrays of Block-like Electronic Components," *International Journal of Heat and Mass Transfer*, Vol. 26, 1983, pp. 689–699.
- ⁴Sparrow, E. M., Yanezmoreno, A. A., and Otis, D. R. Jr., "Convective Heat Transfer Response to Height Differences in an Array of Block-like Electronic Components," *International Journal of Heat and Mass Transfer*, Vol. 27, No. 3, 1984, pp. 469–473.
- ⁵Sogin, H. H., "Sublimation from Disks to Air Streams Flowing Normal to Their Surfaces," *Transactions of the ASME*, Vol. 80, 1958, pp. 61–71.
- ⁶Kline, S. J. and McClintock, F. A., "Describing Uncertainties in Single-Sample Experiments," *Mechanical Engineering*, Vol. 75, Jan. 1953, pp. 3–8.
- ⁷Nogueira Dos Santos, W. F., "Escoamento interno de ar sobre uma matriz de módulos retangulares: Efeitos de não-uniformidades na transferência de calor e perda de carga," M.S. thesis, Pontifícia Universidade Católica do Rio de Janeiro, Departamento de Engenharia Mecânica, Rio de Janeiro, Brazil, 1985.

Notice to Subscribers

We apologize that this issue was mailed to you late. As you may know, AIAA recently relocated its headquarters staff from New York, N.Y. to Washington, D.C., and this has caused some unavoidable disruption of staff operations. We will be able to make up some of the lost time each month and should be back to our normal schedule, with larger issues, in just a few months. In the meanwhile, we appreciate your patience.